Common-Path Wavefront Sensing for Advanced Coronagraphs

J. Kent Wallace
Jet Propulsion Laboratory,
California Institute of Technology
4800 Oak Grove Dr.
Pasadena, CA 91109
818-393-7066
James.K.Wallace@jpl.nasa.gov

Eugene Serabyn
Jet Propulsion Laboratory,
California Institute of Technology
4800 Oak Grove Blvd.
Pasadena, CA 91109
818-393-5253
Eugene.Serabyn@jpl.nasa.gov

Dimitri Mawet
European Southern Observatory
Karl-Schwarzschild-Str.2
85748 Garching, Germany
dmawet@eso.org

Abstract—**Imaging of faint companions around nearby stars is not limited by either intrinsic resolution of a coronagraph/telescope system, nor is it strictly photon limited. Typically, it is both the magnitude and temporal variation of small phase and amplitude errors imparted to the electric field by elements in the optical system which will limit ultimate performance. Adaptive optics systems, particularly those with multiple deformable mirrors, can remove these errors, but they need to be sensed in the final image plane. If the sensing system is before the final image plane, which is typical for most systems, then the non-common path optics between the wavefront sensor and science image plane will lead to un-sensed errors. However, a new generation of high-performance coronagraphs naturally lend themselves to wavefront sensing in the final image plane. These coronagraphs and the wavefront sensing will be discussed, as well as plans for demonstrating this with a high-contrast system on the ground. Such a system will be a key system-level proof for a future space-based coronagraph mission, which will also be discussed.**

TABLE OF CONTENTS

1. INTRODUCTION 1
2. FIRST ORDER PROPERTIES OF STELLAR CORONAGRAPHS 1
3. AN IMPROVED CORONAGRAPH 3
4. IMPROVED WAVEFRONT SENSING 4
5. AN ARCHITECTURE FOR INTEGRATED WAVEFRONT SENSING AND CORONAGRAPHY 6
6. FUTURE UPGRADES 6
8. CONCLUSION 7
9. ACKNOWLEDGEMENTS 7
REFERENCES 7
BIOGRAPHY 7

1. INTRODUCTION

With well over a thousand exoplanets detected to date from both ground and space, one might think the area is quite mature. However, few of these planets have been detected directly, and for those that have been detected directly, as yet none have been characterized spectrally. Therefore, direct detection of faint companions, like planets, around nearby stars is a rich and active area of science and engineering. Indeed, a new class of ground-based exoplanet-finding instruments are about to be commissioned (P1640, GPI, SPHERE) which share the common goals of direct detection and spectroscopy.

Surprisingly, a space-based mission with the same goals as these ground-based instruments of detection and characterization would be limited by the same effects: the temporal variation of wavefront errors (both amplitude and phase) during a long science exposure. If this source of high-contrast limitation can be successfully resolved on the ground, it would also provide a clear demonstration of how to architect systems for future space missions.

Steady progress in coronagraph development has continued since the first generation of direct-imaging instruments was conceived. In this intervening period, a new class of phase-only, image-plane coronagraph has evolved: the vector vortex coronagraph. The vector vortex benefits from: simple implementation, high throughput, and very small inner working angle. Recently, however, a dual-stage implementation has been developed which provides a very clean and simple means of dealing with the diffraction (and loss of contrast) from apertures with central obscurations.

This architecture also leads to a simple method of sensing the electric field of the speckles in the final image plane. Sensing these speckles directly, and in the final image plane minimizes the absolutely removes the effect of non-common path errors. By using the coherent starlight that has been rejected by coronagraph, both the amplitude and phase of these image plane speckles are directly sensed in broadband light.

The combination of advanced coronagraph architecture and direct, common-mode speckle sensing leads to a system that is nearly optimized for breaking through the barriers that currently limit contrast. The architecture can be readily adopted for a future space mission.

2. FIRST ORDER PROPERTIES OF STELLAR CORONAGRAPHS

I begin with a brief discussion of the first order properties of stellar coronagraphs. A nearly exhaustive comparison of different varieties of coronagraphs, with their merits and shortcomings, has been described elsewhere. Here, however, I simply summarize the first order properties and emphasize

978-1-4577-0557-1/12/$26.00 ©2012 IEEE

the impact and static and dynamic errors on the stellar electric field, and the resulting impact on final contrast.

The electric field immediately before the input pupil is given by:

$$E(u,v) = P(u,v) \cdot A(1+\varepsilon(u,v))e^{i\varphi(u,v)} \qquad (1)$$

Here, the pupil function is given by *P(u,v)*, the mean electric field amplitude is A, the point-by-point variation in the electric field strength is given by *ε(u,v)*. The pupil-dependent phase is given by *ϕ(u,v)*. For simplicity sake, let's first assume that the phase in the input pupil is small, compared to a radian. With this assumption the expression for the electric field then becomes:

$$\begin{aligned} E(u,v) &\approx P(u,v) \cdot A(1+\varepsilon(u,v)(1+i\varphi(u,v))) \\ E(u,v) &\approx P(u,v) \cdot A(1+\varepsilon(u,v)+i\varphi(u,v)+i\varepsilon(u,v)\varphi(u,v)) \\ E(u,v) &\approx P(u,v) \cdot A(1+\varepsilon(u,v)+i\varphi(u,v)) \end{aligned} \qquad (2)$$

Here, the second order terms have been dropped. This field is propagated to the focal plane of the system by a Fourier transform. This Fourier transform operator is shown schematically as F[]:

$$E(\eta,\upsilon) = F[P(u,v)] * F[A(1+\varepsilon(u,v)+i\varphi(u,v))]$$

$$E(\eta,\upsilon) = A\ PSF(\eta,\upsilon) * \left\{ \begin{matrix} \delta(\eta,\upsilon)+ \\ F[\varepsilon(u,v)+i\varphi(u,v)] \end{matrix} \right\}$$

$$\begin{aligned} E(\eta,\upsilon) &= A\ PSF(\eta,\upsilon) + A\ PSF(\eta,\upsilon) * \\ &F[\varepsilon(u,v)+i\varphi(u,v)] \end{aligned} \qquad (3)$$

where the Cartesian coordinates in the image plane are represented by η, ν and the convolution operation is represented by the * symbol. The Fourier transform of the pupil function is represented by PSF. The electric field in the image plane is therefore given by the sum of two terms, the first is the PSF of the system with a perfect input field (no phase or amplitude errors). The second term is given by the convolution of this PSF with the Fourier transform of the phase and amplitude errors of the input beam.

The action of the coronagraph can most simply be expressed as the removal of the first term in equation 3. Although a hard-edged focal plane mask coronagraph (for instance) does not extend outwards indefinitely as does the PSF, the approximation still provides insight. The electric field immediately after the focal plane mask is then approximated as:

$$E(\eta,\upsilon) = A\ PSF(\eta,\upsilon) * F[\varepsilon(u,v)+i\varphi(u,v)] \qquad (4)$$

Another Fourier transform will take us back to the Lyot pupil. The Cartesian coordinates are represented by (x, y) in the re-imaged plane.

$$F[E(\eta,\upsilon)] = E(x,y) = F[A\ PSF(\eta,\upsilon) * F[\varepsilon(u,v)+i\varphi(u,v)]]$$

$$E(x,y) = A\,P(x,y) \cdot (\varepsilon(x,y)+i\varphi(x,y)) \qquad (5)$$

The electric field from the original input pupil has been modified in the Lyot pupil in following way: the DC part of the electric field has been removed, and the electric field that remains is composed of a real part due to amplitude errors and an imaginary part from phase errors.

To determine the E-field in the final image plane, another Fourier transform is performed. Beforehand, we express both the amplitude and phase in their symmetric (even) and anti-symmetric (odd) forms.

$$\varepsilon = \sum_f \varepsilon_{e,f} Cos(\bar{x}\ f) + \varepsilon_{o,f} Sin(\bar{x}\ f)$$

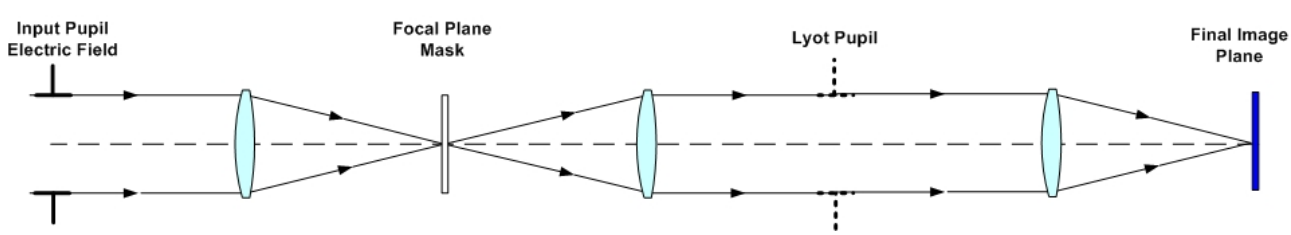

Figure 1 – This is a simple optical layout of canonical Lyot coronagraph. Light enters from the left at the input pupil. The lens forms an image at the location of the focal plane mask. Light then propagates from the focal plane mask to the second lens which forms the Lyot pupil. From this pupil the final image is formed by the third lens. This single-stage optical coronagraph captures the fundamental operation of a coronagraph on starlight.

978-1-4577-0557-1/12/$26.00 ©2012 IEEE

$$\varphi = \sum_f \varphi_{e,f} Cos(\bar{x}\, f) + \varphi_{o,f} Sin(\bar{x}\, f) \qquad (6)$$

The decomposition of the phase and amplitude into even and odd components given by Eq. 6 will be a useful tool in the expression of the intensity in the final image plane. Here, the Cartesian coordinates *x, y* have been replaced by the vector representation $\bar{x}$. The electric field in the pupil plane from equation 5 can then be expressed as follows:

$$E(\bar{x}) = A\,P(\bar{x}) \cdot \begin{pmatrix} \sum_f \varepsilon_{e,f} Cos(\bar{x}\, f) + \varepsilon_{o,f} Sin(\bar{x}\, f) + \\ i \sum_f \varphi_{e,f} Cos(\bar{x}\, f) + \varphi_{o,f} Sin(\bar{x}\, f) \end{pmatrix} \qquad (7)$$

The electric field in the final image plane is then given by another Fourier Transform.

$$F[E(\bar{x})] = A\,F[P(\bar{x})] * F\left[\begin{pmatrix} \sum_f \varepsilon_{e,f} Cos(\bar{x}\, f) + \varepsilon_{o,f} Sin(\bar{x}\, f) + \\ i \sum_f \varphi_{e,f} Cos(\bar{x}\, f) + \varphi_{o,f} Sin(\bar{x}\, f) \end{pmatrix}\right] \qquad (8)$$

The above expression is re-written to combine: 1) the even amplitude errors with the odd phase errors and 2) the odd amplitude errors with the even phase errors. This is done because for condition 1) the resulting image plane E-field components are both real and for condition 2) they are both imaginary.

$$E(\bar{f}) = A\,PSF(\bar{f}) * F\left[\begin{pmatrix} \sum_{f_i} \varepsilon_{e,f} Cos(\bar{x}\, f_i) + i\varphi_{o,f} Sin(\bar{x}\, f_i) + \\ \sum_{f_i} \varepsilon_{o,f} Sin(\bar{x}\, f_i) + i\varphi_{e,f} Cos(\bar{x}\, f_i) \end{pmatrix}\right] \qquad (9)$$

By expanding the Fourier Transform operation, we arrive at the following expression for the image plane E-field.

$$E(\bar{f}) = A\,PSF(\bar{f}) * \begin{pmatrix} \sum_{f_i} \left(\left(\varepsilon_{e,f} - \varphi_{o,f}\right) + i\left(\varepsilon_{o,f} + \varphi_{e,f}\right)\right) \delta(f - f_i) + \\ \sum_{f_i} \left(\left(\varepsilon_{e,f} + \varphi_{o,f}\right) - i\left(\varepsilon_{o,f} - \varphi_{e,f}\right)\right) \delta(f + f_i) \end{pmatrix} \qquad (10)$$

The final image plane can therefore be described in the following way: it is composed of a series of delta functions that are symmetric about the focal plane. The delta functions have magnitudes that are composed of real and symmetric parts. For the positive spatial frequency space ($\delta(f - f_i)$), the real part is the difference between the symmetric part of the amplitude error and antisymmetric part of the phase error. The imaginary part is given by the sum of the anti-symmetric part of the amplitude error and the symmetric part of the phase error. For the negative spatial frequency, the difference is replaced with a sum, and the sum with a difference, and the imaginary part changes sign. These delta functions are then convolved by the point response of the telescope given by the PSF.

The job of the coronagraph is to insure that the DC part of the stellar light has been sufficiently rejected (removal of the first term in equation 3). This must be done in such a way as to maintain high throughput, provide a small inner working angle and also retain the full telescope resolution.

After the coronagraph has done this work, in order to maintain high contrast the amplitude and phase errors in the system must be made small. However, once they are made small they must stay small. Temporal variation of the phase and amplitude errors must either be keep to a minimum, or these speckles (both the real and imaginary parts) must be sensed and controlled with active elements (such as a deformable mirror). The temporal evolution of these speckles will limit the contrast of both space based and ground based high-contrast instruments. Successfully demonstrating how to address these issues is key to achieving ultimate performance.

The next section will describe a new class of coronagraph that addresses the issues of: high throughput, small inner working angle, and high resolution. An improved architecture shows how these are well suited to telescopes with central obscurations.

The subsequent section will describe a means for doing the wavefront sensing that is necessary to both: 1) quantify the speckles that limit contrast and 2) actively track their temporal evolution.

The final section will describe our plans for integrating these two key elements (advanced coronagraphy and advanced wavefront sensing) into a new high-contrast instrument for Palomar. This instrument will provide a system level, end-to-end demonstration of a high-contrast instrument that is equally suitable for space.

3. AN IMPROVED CORONAGRAPH

The vector vortex, among all the varieties of coronagraphs, has some very nice properties. It is a phase only coronagraph used in the image plane, and therefore has high throughput. It also benefits from a small inner working angle, as small as 1 λ/D. This coronagraph is easy to implement and has been successful in demonstrating direct detection of faint companions around nearby objects.

978-1-4577-0557-1/12/$26.00 ©2012 IEEE

However, with all of these benefits, it does suffer from one drawback: it is not well suited to a telescope with a central obscuration.

For an aperture without a central obscuration, the vector vortex will move the light that is on-axis to a location immediately outside the geometric pupil at the Lyot plane. The interior of the pupil, however, is left completely dark. This bright ring of light outside the geometric pupil is rejected with a circular pupil stop.

For a system with a central obscuration, light on axis is still moved to outside the geometric pupil. However, light at the secondary pupil is moved interior to the otherwise dark area of the pupil for the un-obscured system. Because this light is diffuse, it is difficult to reject. A hard edge stop at the Lyot pupil will only have the effect of blocking light exterior to the pupil. The resulting contrast in the final image plane is dominated by a broad illumination pattern (Figure 2.)

The pupil illumination after the pupil stop in the Lyot plane nearly resembles the illumination for an un-obscured pupil. One can image that by reversing the beam propagation for this portion only, that the light would again be concentrated within a fully illuminated pupil (in this case, the secondary obscuration).

Incredibly, that is indeed the case. By adding another vector vortex in the focal plane after the first Lyot stop, and propagating to a second Lyot stop, light is concentrated at the geometric location of the secondary obscuration. The second vortex has the property that its phase spin is in the opposite clocking as the first vector vortex, but this can be accomplished by flipping it front to back. The light now concentrated in the secondary obscuration is very easily blocked with a hard-edged stop sized to the original central obscuration. Some light does remain interior to the original pupil, however it has been reduced in electric field magnitude by $(a/A)^2$, and the intensity is reduced by $(a/A)^4$. The resulting point spread function for the on-axis light in the final image plane is identical to the original input point spread function except it has been reduced by this ratio. The off-axis light has not been affected at all.

The simplicity of this coronagraph is evident: a couple of transmissive elements in a focal plane. It now affords the possibility of using an on-axis telescope which can greatly simplify the cost of the collecting aperture for a space mission. Other coronagraphs are sensitive to the effect of pupil obscurations, so this tandem-vortex coronagraph is a distinguishing characteristic setting it apart from other coronagraphs.

4. Improved Wavefront Sensing

In the previous section a tandem-vortex coronagraph was presented which addressed the issue of effective starlight suppression for high-contrast imaging. Phase and amplitude errors in the system will still limit contrast if not dealt with effectively. Ideally these errors would be sensed directly in the final image plane where they have the most immediate impact on contrast. The sensing technique would permit the measurement of the full electric field (both real and

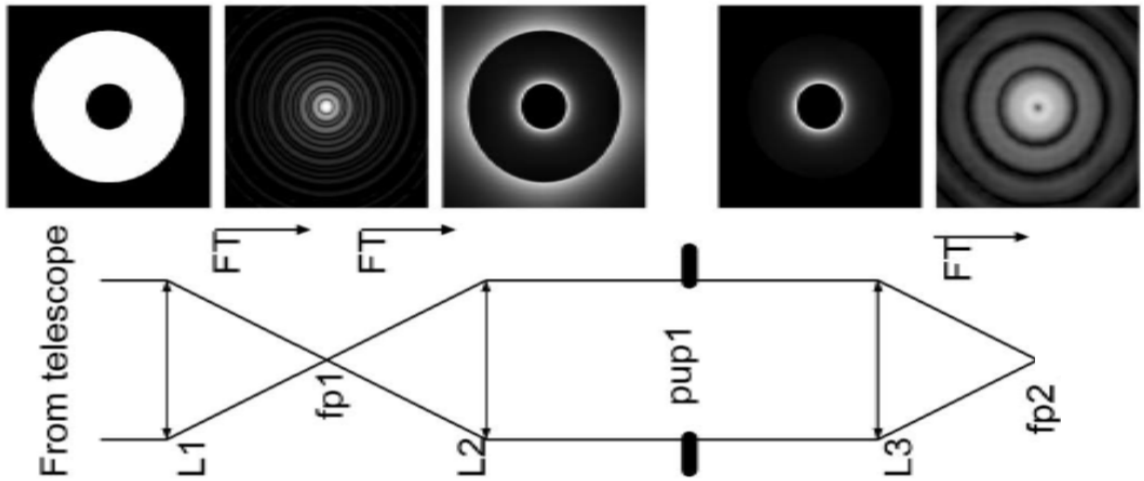

Figure 2 – This image shows the effect of an input aperture with a central obscuration on the single-stage vector vortex coronagraph. The pupil and image plane intensities are illustrated in the series of images at the top of the diagram. The schematic below these images shows their relative location in the optical relay. This coronagraph leads to excess light around the secondary obscuration that is not easily removed.

978-1-4577-0557-1/12/$26.00 ©2012 IEEE

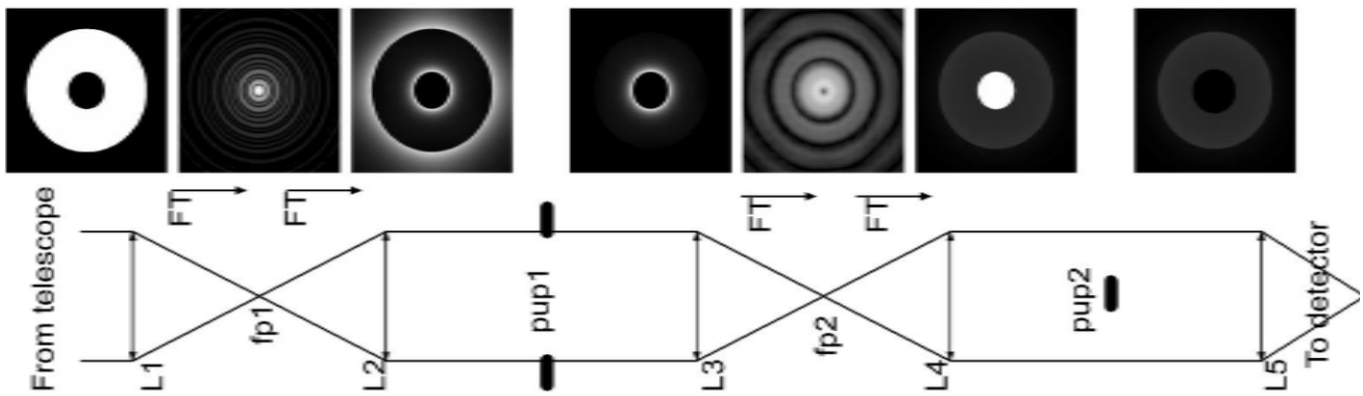

Figure 3 – This diagram illustrates the response of an input aperture with a central obscuration as it passes through a tandem-vortex coronagraph. Similar to previous figure, the images represent the intensities in the various pupil and image planes in the system. The diagram below these images represent the optical system in a schematic way. This tandem-vortex architecture is very effective at removing the effect of the secondary obscuration from the system. The final integrated intensity is reduced by the ratio $(a/A)^4$, where a is the secondary obscuration diameter and A is the primary pupil diameter.

imaginary parts) such that corrective action could be taken to mitigate their effects. It turns out that the tandem-vortex described above naturally lends itself to this method of image-plane wavefront sensing.

The light that is concentrated in the secondary obscuration at the second Lyot stop can be used to provide a reference beam. This light is coherent with light scattered to the final image plane. If we allow a very small portion of this light to be propagated to the final image plane, it provides a reference beam that interferes with the image plane speckles. If, for instance, a point light part was used in this plane (the remaining light being rejected), it would act as a spherical wave and diffract outwards. After the imaging lens, it would create a near-uniform distribution of light in the image plane.

By making the second Lyot stop a reflective mirror, it's feasible to use in this small area a phase-shifting micro-mirror that is centered on the secondary obscuration. The phase diversity that can induced into this reference beams permits phase-shifting interferometry techniques to be applied. In this way, both the real and imaginary parts of the image plane speckles can be estimated directly.

The observation scenario would proceed as follows: first, the star is aligned to be boresited to the tandem vortex, second, the phase-shifting micro-mirror is unblocked using a shutter or iris, third, an estimate of the image plane speckles are made with interferometric sensing in the image plane, fourth, corrections are made to optimize contrast over a

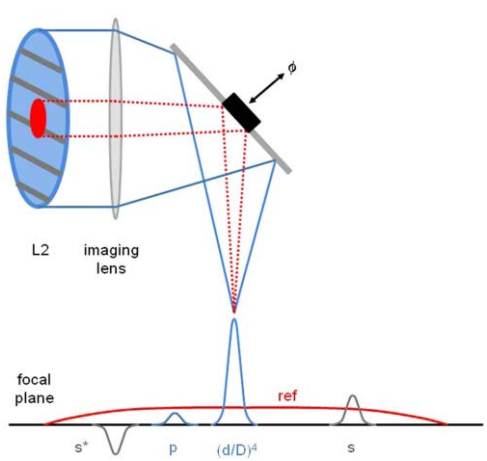

Figure 4 – This diagram represents the use of the light in the secondary obscuration of the tandem-vortex coronagraph to introduce a reference beam. The small micro-mirror at the center of the fold mirror will impart a phase-shift to the reference light. In the final image plane, this reference light forms a broad beam. Demodulation of the resulting interference pattern allows one to estimate the full electric field of the speckles in the final image plane.

978-1-4577-0557-1/12/$26.00 ©2012 IEEE

portion of the image plane, fifth, the micro-mirror is shuttered to prevent scattered light and finally, science observations begin with this ultimate contrast. This procedure can be repeated on timescales over which the speckles have again evolved to the point where contrast is impacted.

This sensing is done common-mode, broadband and measures speckle electric-field directly in the final image plane.

5. An Architecture for Integrated Wavefront Sensing and Coronagraphy

With these two improvements to high contrast imaging in hand, we are progressing with an integrated tandem-vortex coronagraph and image-plane speckle sensor to be deployed at the Hale telescope at Mount Palomar. This new coronagraph will employ the tandem-vortex as described above to properly deal with the secondary obscuration. It will also use the phase-shifting micro-mirror in the secondary obscuration in the second Lyot pupil to introduce the phase-shifted reference beam.

A preliminary schematic of this architecture is shown below. Light enters from the telescope and adaptive optics system from the lower right. It first passes through a couple of fold mirrors to insure proper pointing and pupil stability. The light is re-collimated with an off-axis parabola. A pair of alignment mirrors insure proper registration of the vector-vortex and the stellar image. After the first Lyot pupil, another pair of alignment mirrors again insures the proper degrees of freedom for the second stage of the coronagraph. The second Lyot pupil is partially reflective and partially opaque. The reflective areas correspond to the clear parts of the original input pupil and the small phase-shifting micro-mirror. The occulting parts are the vast majority of the secondary obscuration save the small micro-mirror.

With this system we hope to demonstrate the requisite star-light suppression and image-plane speckle sensing and control to achieve contrast that is limited only by photon noise, and limited by the time variability of phase and amplitude errors. If we can achieve this, then we will have demonstrated a end-to-end system that is limited by same instrument in space.

6. Future Upgrades

Our plan is to have a nominally operating system working on the sky by the fall of 2012. However, there are further improves that can be made for ultimate performance. After this first year, we plan on adding atmospheric dispersion compensators to remove the chromatic atmospheric refraction. We also envision picking off part of the light immediately before the science focal plane to feed another wavefront sensing camera. This camera would act as the surrogate for the science image plane, but it would sense and control the phase and amplitude errors as they evolve, thus allowing the science camera to stare for much longer periods

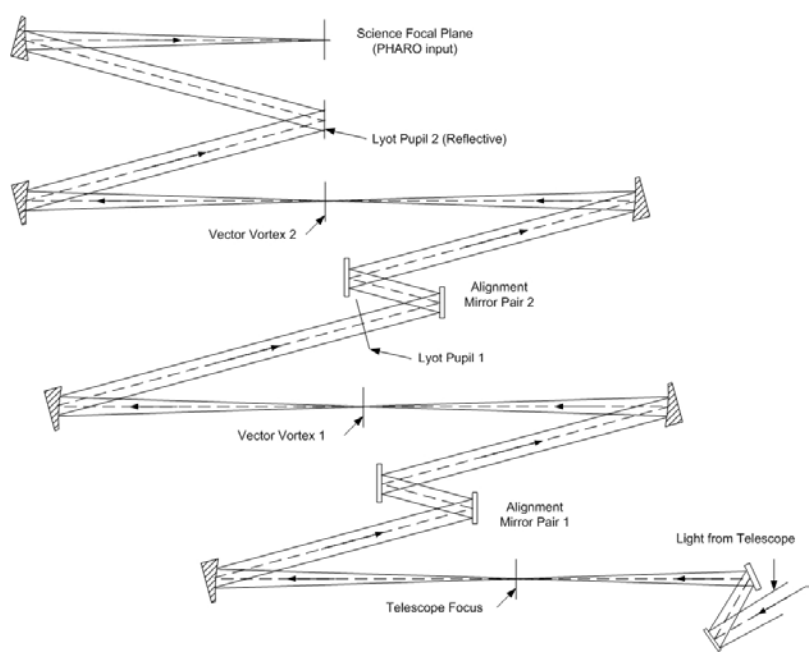

Figure 5 – This schematic layout shows our plans for implementing both the tandem-vortex and wavefront sensing ideas into a stellar coronagraph instrument for the Hale telescope at Palomar Observatory. This optical configuration captures a few of the key functionalities that will be required in the final system. Alignment mirrors are added internal to the beam path to insure proper alignment of the system.

978-1-4577-0557-1/12/$26.00 ©2012 IEEE

of time. With these improves the system should achieve ultimate performance.

8. CONCLUSION

Recent advancements in the coronagraph and wavefront sensing architectures lend themselves to elegant and simple high-contrast system. These systems will not be limited by: residual atmospheric phase and amplitude errors, or by time-varying speckles in the image plane. Instead contrast will be limited by photon noise, and thereby achieve ultimate contrast. We are in the process of building such a system for the Palomar Observatory. It will provide a persuasive demonstration that key systems-level issues have been addressed and resolved.

9. ACKNOWLEDGEMENTS

This work was carried out by the Jet Propulsion Laboratory, California Institute of Technology, under contract with the National Aeronautics and Space Administration.

REFERENCES

[1] exoplanet.eu/catalog.php

[2] B. MacIntosh, et.al., "The Gemini Planet Imager: from science to design to construction", Proc. SPIE **7015**, (2008).

[3] J.-L. Beuzit, et al., "SPHERE: a 'Planet Finder' instrument for the VLT", Proc. SPIE **7014**, (2008).

[4] S. Hinkley, B.R. Oppenheimer, D.S. Brenner, A. Sivaramakrishnan, R. Roummer, I.R. Parry, and D.L. King, "A new integral field spectrograph for exoplanetary science at Palomar", Proc. SPIE **7015**, (2008).

[5] D. Mawet, et. al., "Optical Vectorial Vortex Coronagraph using Liquid Crystal Polymers: theory, manufacturing, and laboratory demonstration", Optics Express, **17**, pp. 1902-1918, (2009).

[6] D. Mawet, B. Mennesson, E. Serabyn, K. Stapelfeldt, and O. Absil, "A Dim Candidate Companion to ε Cephei", ApJ Letters, **738**, (2011).

[7] D. Mawet, et. al. "Improved high-contrast imaging with on-axis telescopes using a multistage vortex coronagraph", Opt. Lett., **36**, pp. 1506-1508 (2011).

[8] E. Serabyn., J.K. Wallace, and D. Mawet, "Speckle-phase measurement in a tandem-vortex coronagraph", Applied Optics, **50**, pp. 5453 – 5456 (2011).

[9] A. Give'on, B. Kern, S. Shaklan, D. Moody and L. Pueyo, "Broadband wevefront correction algorithm for high-contrast imaging systems", Proc. SPIE **6691**, (2007).

[10] O. Guyon, E.A. Pluzhnik, M.J. Kuchner, B. Collins, and S.T. Ridgway, "Theoretical limits on the extrasolar terrestrial planet detection with coronagraphs", Astrophys. J. Suppl. Ser. **167**, 81-99 (2006).

[11] A. Shivaramakrishnan, et.al, "Ground-based Coronagraphy with High Order Adaptive Optics", AstroPh, (2001)

BIOGRAPHY

Kent Wallace *is a Senior Optical Engineer at the Jet Propulsion Laboratory. He has been involved in the design and development of several ground based instruments including the Palomar Testbed Interferometer, the Keck Interferometer and the Palomar Adaptive Optics System. His interest over the past few years has been nulling interferometry, optical communications, and wave front sensing. He has a BS in Physics from Rose-Hulman Institute of Technology (in beautiful, suburban Terre Haute, IN) and a MS in Optics from the University of Rochester.*

978-1-4577-0557-1/12/$26.00 ©2012 IEEE

978-1-4577-0557-1/12/$26.00 ©2012 IEEE